Effects of Conductor Edge Profile on Transmission Properties of Conductor-Backed Coplanar Waveguides

Lei Zhu, *Member, IEEE,* and Eikichi Yamashita, *Fellow, IEEE*

Abstract—**A boundary integral equation method is applied to the full-wave analysis of conductor-backed coplanar waveguides with a rectangular or trapezoidal conductor cross-section. Due to a particular choice of Green's functions for each subregion defined in a given cross-section, electromagnetic fields in each subregion are analytically expressed in terms of equivalent magnetic currents on apertures and resulting integration contours are defined only on aperture surfaces. Consequently, this approach can overcome relative convergence problems even in the case of largely different aperture widths among subregions. Numerical data show that this approach has a stable convergence property and requires a short computation time. Numerical results obtained with this approach are in excellent agreement with other available theoretical data. A series of calculated data for some rectangular and trapezoidal conductor configurations are provided to show the effects of conductor edge profile on transmission properties of conductor-backed coplanar waveguides.**

I. Introduction

PLANAR TRANSMISSION LINES were extensively studied theoretically and experimentally for many years [1]. The coplanar waveguide was proposed by Wen [2] as a promising planar transmission line which was made of a central strip with two ground planes on the same surface of a substrate. For heat removal from practical devices, an additional ground plane is placed on the other surface of the substrate. This makes up a conductor-backed coplanar waveguide (CBCPW) [3]. Its transmission properties have been analyzed using the spectral domain method [3], [4], and the transverse resonance method [5].

As for the CBCPW structure with finite metallization thickness, the transverse resonance method is a typical numerical method for the full-wave analysis of its transmission properties. A serious relative convergence problem, however, was found with the application of the transverse resonance method and it was treated by many scholars using varied processes [5]–[8]. The above-mentioned problem can be reduced to some extent by using an improved transmission-matrix formulation [7] and a scattering-type transverse resonance technique [5], [6].

Recently, an extended and a mixed spectral domain method, which were essentially the same, were proposed by Kitazawa *et al.* [4], [9] and Chan *et al.* [10], respectively, to analyze the properties of planar transmission lines with or without finite metallization thickness. These methods use spectral dyadic Green's functions for each subregion defined in a given cross-section to express electromagnetic fields in each subregion. These approaches may be able to overcome the relative convergence seen in the standard transverse resonance method, but may add more analytical manipulations such as complicated Fourier transforms.

In a previous paper, the authors reported the eigenfunction weighted boundary integral equation method for the full-wave analysis of various planar transmission lines with finite metallization thickness [11]. Although the eigenfunctions are simpler than Green's functions, longer computation time and relative convergence problems can not be avoided in the case of an extremely large ratio of aperture widths among subregions.

In this paper a new boundary integral equation method [12] is applied for the study of the transmission properties of conductor-backed coplanar waveguides which uses Green's functions, the Green's identity, and the equivalence principle. In comparison with varied transverse resonance techniques combined with the mode-matching procedure where the numerical expansion of hybrid fields are performed in each rectangular subregion [5], [6], numerical processes of the present procedure is limited only on each aperture between two adjacent subregions because of a special choice of Green's functions which is satisfied with homogeneous boundary conditions of each rectangular subregion. In short, the resultant matrix is only related to the expansion of aperture fields not to that of regional fields so that the present procedure is superior to the above-mentioned technique in the computational efficiency and accuracy for structures including an extremely large difference of subregion widths.

The major difference between the present approach and the mixed spectral domain method is that the Green's functions are set up in the space domain in the present method which, therefore, can be extended to handle the transmission lines with arbitrary cross sections similarly to the quasi-TEM analysis using the boundary element method [13].

As a consequence of current trends in MMIC's toward higher frequencies and higher component densities, the effects of conductor thickness and conductor edge profile can not be neglected anymore due to narrower strip widths of microstrip lines [14], [15], narrower slot apertures of CPW's, and underetching and electrolytical growth in the fabrication

Manuscript received October 28, 1993; revised July 25, 1994.

The authors are with the University of Electro-Communications, Chofu, Tokyo, Japan 182.

IEEE Log Number 9408567.

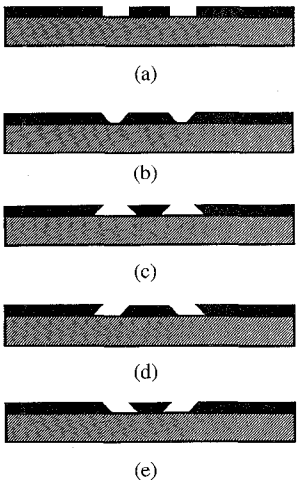

Fig. 1. Cross-sectional geometry of CBCPW's with rectangular or trapezoidal conductor cross-sections.

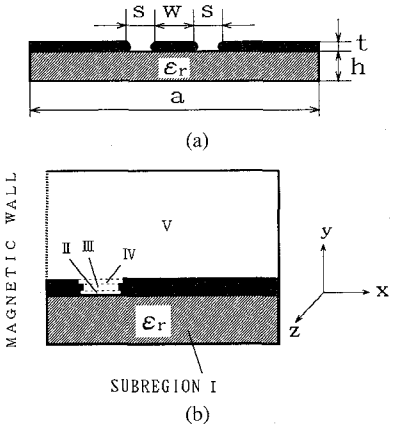

Fig. 2. Cross-sectional geometry of a CBCPW with arbitrary conductor edge profile. (a) Cross-sectional geometry. (b) A half of the cross-section to be analyzed.

process. In this paper, we will especially focus our attention to the effects of rectangular and trapezoidal conductor cross sections on the transmission properties of microstrip lines and conductor-backed CPW's. A series of numerical results are provided to show such important effects.

II. Analysis Method

In the previous publications [16], the free-space Green's function was generally chosen as an auxiliary function in the boundary integral equation approach. In the analysis of arbitrary cross-sections, the free-space Green's function and the whole-region Green's function were used to analyze the propagation properties of microstrip lines with finite metallization thickness [17] and a trapezoidal transmission line [13] based on the quasi-TEM wave approximation, and a microstrip line with arbitrary cross section based on the rigorous full-wave analysis [14] where boundary integrations were defined on conductor surfaces using the Green's function satisfying the field continuity at substrate interface. As for coplanar waveguides consisting of a wide conductor surface and a narrow aperture surface, boundary integration contours should be shortened and limited only on aperture surfaces by choosing suitable Green's functions.

Fig. 1 shows the cross-section of conductor-backed coplanar waveguides (CBCPW's) with rectangular and trapezoidal conductor strips of five kinds. Fig. 1(a) is a typical model discussed in the previous analysis, and the other four kinds of cross-sections as shown in Fig. 1(b)–(e) are profiles approximating some modifications caused by underetching or electrolytical growth during the fabrication. Fig. 2(a) shows a cross-section of CBCPW with an arbitrary conductor edge profile. According to the symmetry of this structure, only a half of the cross-section is taken into account in the analysis. Since the magnitude of electromagnetic fields can be negligible at a far away point from the central strip and the edge of the ground conductors, an electric or magnetic wall at a far point from the symmetrical plane is assumed to exist for speeding up the series convergence of Green's functions. In addition, any arbitrary configuration of aperture subregions can be decomposed into rectangular subregions as shown in Fig. 2(b) of the half cross-section.

The half cross-section is divided into five uniform subregions with rectangular configurations as shown in Fig. 2(b). Like the transverse resonance method, electromagnetic fields in each subregion are written as a superposition of the TM-mode and the TE-mode propagating in the z-axis. The difference between the transverse resonance method and the present method is that the analytical Green's functions satisfying the boundary conditions of rectangular subregions are chosen as field expressions of the TM-mode and the TE-mode for each subregion in the present method while approximate mode summations are chosen in the case of the transverse resonance method. The Green's identity of the second kind is written as

$$\int\int_S [G(r,r_S)\nabla_\perp^2\Phi(r_S) - \nabla_\perp^2 G(r,r_S)\Phi(r_S)]dS = \int_\Gamma [G(r,r_S)\frac{\partial\Phi(r_S)}{\partial n_S} - \frac{\partial G(r,r_S)}{\partial n_S}\Phi(r_S)]d\Gamma \quad (1)$$

which results in fields in each subregion expressed in terms of fields on the aperture of each subregion as follows:

$$E_z(r) = -\int_{\text{aperture}} \frac{\partial G^e(r,r_S)}{\partial n_S} E_z(r_S)dl_S \quad (2a)$$

$$H_z(r) = \int_{\text{aperture}} G^h(r,r_S)\frac{\partial H_z(r_S)}{\partial n_S}dl_S \quad (2b)$$

where G^e and G^h denote the two kinds of Green's functions corresponding to the TM-mode and the TE-mode, respectively. The symbols, r and r_s denote the field position and the source position, respectively.

In order to conveniently utilize the tangential continuity of fields on each aperture between two adjacent subregions, it is necessary to transform the above normal differentiation terms to tangential components and tangential differentiation terms. Consequently, the following relations are derived by means of a simple decomposition of Maxwell's equations as

$$H_x = \frac{j\omega\varepsilon}{k_c^2}\frac{\partial E_z}{\partial y} - \frac{j\beta}{k_c^2}\frac{\partial H_z}{\partial x} \quad (3a)$$

$$\frac{\partial H_z}{\partial y} = -\frac{k_c^2}{j\omega\mu}E_x - \frac{\beta}{\omega\mu}\frac{\partial E_z}{\partial x} \tag{3b}$$

where

$$k_c^2 = \omega^2\mu\varepsilon - \beta^2. \tag{4}$$

Substituting (3) into (2) and carrying out some transformations of differentiation terms, the magnetic fields in each subregion are expressed in terms of the tangential electric fields on the apertures, E_x and E_z, and analytical Green's functions in the following form:

$$H_x = \int_{\text{aperture}} [G_{11}E_x + G_{12}E_z]dx_S \tag{5a}$$

$$H_z = \int_{\text{aperture}} [G_{21}E_x + G_{22}E_z]dx_S \tag{5b}$$

where G_{11}, G_{12}, G_{21}, and G_{22} are the four terms of the space dyadic Green's function which are written as

$$G_{11} = \beta\sum_m \frac{\partial G_m}{\partial x} \tag{6a}$$

$$G_{12} = \sum_m \frac{\omega^2\mu\varepsilon - k_{xm}^2}{k_{xm}^2}\frac{\partial^2 G_m}{\partial x \partial x_S} \tag{6b}$$

$$G_{21} = k_c^2\sum_m G_m \tag{6c}$$

$$G_{22} = \beta\sum_m \frac{\partial G_m}{\partial x_S} \tag{6d}$$

where

$$G_m = -\frac{2}{ak_{ym}}\frac{\phi(x)\phi(x_S)}{\sin(k_{ym}h)} \begin{cases} \cos[k_{ym}(y-h)]\cos(k_{ym}y_S) & (y > y_S) \\ \cos(k_{ym}y)\cos[k_{ym}(y_S - h)] & (y < y_S) \end{cases} \tag{7}$$

and

$$\phi(x) = \begin{cases} \sin(k_{xm}x) & (m = 1, 2, \ldots, \infty) \\ & \text{(in subregion I, V)} \\ \cos[k_{xm}(x - w/2)] & (m = 0, 1, \ldots, \infty) \\ & \text{(in subregion II, III, IV)} \end{cases} \tag{8}$$

$$k_{xm} = \begin{cases} \frac{(2m-1)\pi}{2a} & (m = 1, 2, \ldots, \infty) \quad \text{(in subregion I, V)} \\ \frac{m\pi}{s} & (m = 0, 1, \ldots, \infty) \quad \text{(in subregion II, III, IV)} \end{cases} \tag{9}$$

$$k_{ym} = \sqrt{\omega^2\mu\varepsilon - \beta^2 - k_{xm}^2}. \tag{10}$$

The magnetic fields as expressed in (5) are defined on the aperture of various subregions to set up boundary integral equations based on the continuity of tangential magnetic fields. On the other hand, electric fields on the aperture can be replaced by equivalent magnetic surface currents in two opposite directions, M and $-M$, on the two surfaces of perfectly conducting planes, according to the equivalence principle [18]. In the practical computations, the tangential magnetic fields and equivalent magnetic currents on each aperture are expressed in a series form with finite terms. Here, we select simple sine and cosine functions as the basis functions for the magnetic fields and the equivalent magnetic currents on each aperture. The continuity conditions on the aperture between two adjacent subregions are expressed using the Galerkin's method with the same weighting functions as the basis functions in the following integral form:

$$\int_{\text{aperture}} [H_x^+ - H_x^-]w_x dx = 0 \tag{11a}$$

$$\int_{\text{aperture}} [H_z^+ - H_z^-]w_z dx = 0. \tag{11b}$$

Based on the above relations, the equivalent magnetic currents on the aperture of various subregions can be utilized to connect field functions in two adjacent subregions. As for the five rectangular subregions as shown in Fig. 2(b), four pairs of boundary integral equations are formulated sequentially substituting (5) into (11), in which only equivalent magnetic currents on four apertures remain as the unknown functions and other expressions have only the unknown propagation constant. For the sake of simplicity, two pairs of boundary integral equations are written for the cross-section with three subregions, such as CBCPW with a rectangular conductor cross-section as follows:

$$\int_{l_1}\left\{\int_{l_1}[(G_{11}^{\text{I}} + G_{11}^{\text{II}})M_{z1} + (G_{12}^{\text{I}} + G_{12}^{\text{II}})M_{x1}]dx_S - \int_{l_2}[G_{11}^{\text{II}}M_{z2} + G_{12}^{\text{II}}M_{x2}]dx_S\right\}w_{x1}dx = 0 \tag{12a}$$

$$\int_{l_1}\left\{\int_{l_1}[(G_{21}^{\text{I}} + G_{21}^{\text{II}})M_{z1} + (G_{22}^{\text{I}} + G_{22}^{\text{II}})M_{r1}]dx_S - \int_{l_2}[G_{21}^{\text{II}}M_{z2} + G_{22}^{\text{II}}M_{x2}]dx_S\right\}w_{z1}dx = 0 \tag{12b}$$

$$\int_{l_2}\left\{\int_{l_2}[(G_{11}^{\text{III}} + G_{11}^{\text{II}})M_{z2} + (G_{12}^{\text{III}} + G_{12}^{\text{II}})M_{x2}]dx_S - \int_{l_1}[G_{11}^{\text{II}}M_{z1} + G_{12}^{\text{II}}M_{x1}]dx_S\right\}w_{x2}dx = 0 \tag{12c}$$

$$\int_{l_2}\left\{\int_{l_2}[(G_{21}^{\text{III}} + G_{21}^{\text{II}})M_{z2} + (G_{22}^{\text{III}} + G_{22}^{\text{II}})M_{x2}]dx_S - \int_{l_1}[G_{21}^{\text{II}}M_{z1} + G_{22}^{\text{II}}M_{x1}]dx_S\right\}w_{z2}dx = 0 \tag{12d}$$

where l_1 and l_2 denote the aperture widths between the subregion I and II, and the subregion II and III, respectively. The equivalent magnetic currents, M_{x1} and M_{z1}, on the aperture between the subregion I and II, M_{x2} and M_{z2} on the aperture between the subregion II and III can be expressed in a series form using the following basis functions:

$$\phi_x(x_S) = \cos\left[\frac{n\pi}{s}(x_S - w/2)\right] \quad (n = 0, 1, \ldots, \infty) \tag{13a}$$

$$\phi_z(x_S) = \sin\left[\frac{n\pi}{s}(x_S - w/2)\right] \quad (n = 1, 2, \ldots, \infty). \tag{13b}$$

The weighting functions, w_x and w_z, are expressed by the same functions as the basis functions, ϕ_z and ϕ_x, listed

in (13). In numerical calculations, the number of the basis functions and the weighting functions are taken as the same finite number, N, while the number of Green's function terms are selected as the finite number, M, independently from N. The more terms in Green's function series are taken, the more rigorous results are naturally obtained. The increase of the series terms, M, does not lead to any numerical instabilities as seen in the transverse resonance method [5], but makes numerical results more convergent to rigorous solutions.

As a result of the above manipulations, the integral form of (12) can be rewritten as a system of linear homogeneous equations with the order of $4N$ in a matrix form

$$\begin{bmatrix} [A_{11}] & [B_{11}] & [A_{12}] & [B_{12}] \\ [C_{11}] & [D_{11}] & [C_{12}] & [D_{12}] \\ [A_{21}] & [B_{21}] & [A_{22}] & [B_{22}] \\ [C_{21}] & [D_{21}] & [C_{22}] & [D_{22}] \end{bmatrix} \begin{bmatrix} [X_1] \\ [Z_1] \\ [X_2] \\ [Z_2] \end{bmatrix} = [0] \qquad (14)$$

where the symbols, $[X_1]$, $[Z_1]$, $[X_2]$ and $[Z_2]$, denote the unknown sub-matrices corresponding to the unknown coefficients in the equivalent magnetic currents on the two apertures. The unknown propagation constant, β, is included in each of the coefficient sub-matrices, $[A_{ij}]$, $[B_{ij}]$, $[C_{ij}]$, and $[D_{ij}]$.

For the cross-section with the five subregions as shown in Fig. 2(b), linear homogeneous equations with the order of $2(N_1 + N_2 + N_3 + N_4)$ similar to (14) are derived based on the analytical processes, where the symbol, N_j, denotes the number of the basis functions on the j-th aperture.

III. Numerical Results

An generalized program is constructed based on the above-mentioned model and all of numerical computations are performed on a Sun 4 workstation. The convergence properties in the present method are firstly illustrated in Fig. 3 for a conductor-backed coplanar waveguide (CBCPW) with zero-thickness strip conductor in the case of the width ratio of $(a/2)/s = 25$. Fig. 3(a) shows the convergence curve and CPU time with respect to the number of basis functions on the aperture, N, with the term number of Green's function series, $M = 400$. It is found in Fig. 3(a) that convergence speed for the odd number N is much faster than that for the even number N and CPU time is almost proportional to the square of N. From the convergence curve with the number of the basis functions $N = 3$ as shown in Fig. 3(b), we find that CPU time is almost proportional to M and effective dielectric constants converge to accurate values without instability.

Fig. 4 compares the numerical results by the present method with those given in [14] for an open microstrip line with a trapezoidal conductor cross-section with the discrepancy of less than 2.0%. There still exists a small discrepancy between the two results produced by the assumption of two electric walls. Fig. 5 shows that numerical results obtained by the present method are in good agreement with those given in [5] for a conductor-backed coplanar waveguide with a rectangular conductor cross-section.

Compared with the microstrip line, the dispersion property of the conductor-backed coplanar waveguide depends not only on the substrate height and strip width but also on the slot width located on the dielectric interface. Under our present

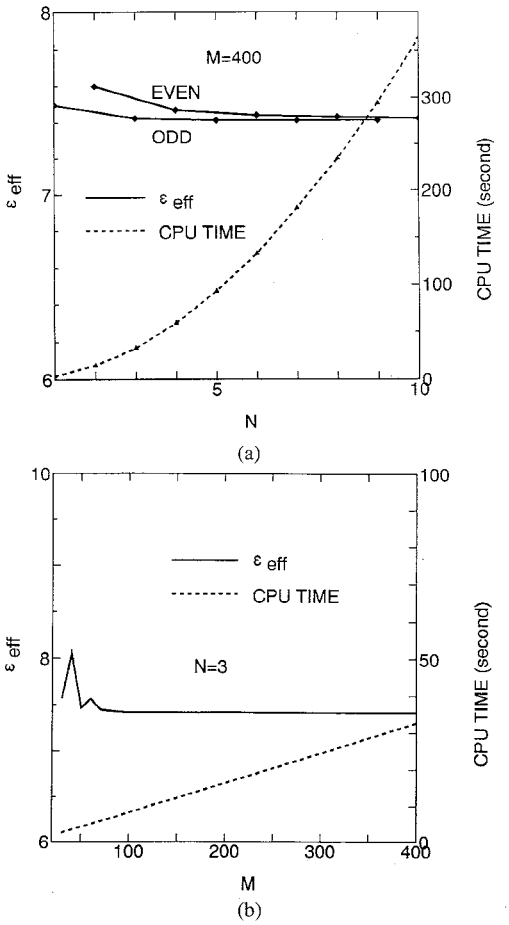

Fig. 3. Convergence properties for a CBCPW with zero-thickness strip conductor ($w = 72.4$ μm, $s/w = 0.5$, $a/w = 25$, $h = 100$ μm, $\varepsilon_r = 12.9$) (a) Number of basis functions and its CPU times. (b) Number of Green's function series and its CPU times.

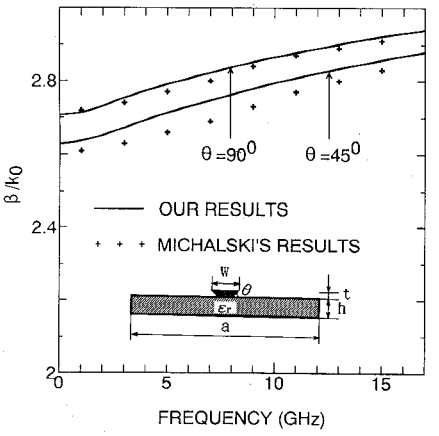

Fig. 4. Comparison of the propagation constants of the microstrip line having a trapezoidal conductor cross-section calculated by the present method with those given in [14] ($w = 3$ mm, $t = 0.3$ mm, $h = 0.635$ mm, $a =$ mm, 15 $\varepsilon_r = 9.8$).

knowledge, any theoretical or experimental report on the entire shape of its dispersion curve has not been published. With the increase of frequencies, conceptually, the effective dielectric constant of the dominant mode tends to the relative permittivity of the dielectric substrate. However, it is difficult theoretically to give a quantitative judgment on the position

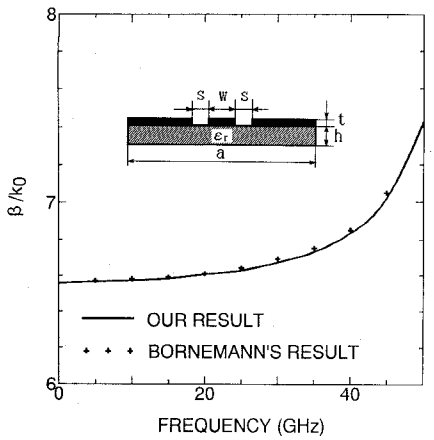

Fig. 5. Comparison of the propagation constants of a CBCPW having finite metallization thickness calculated by the present method with those given by [5] ($2w = s = 80$ μm, $a = 1.2$ mm, $h = 0.3$ mm, $t = 5$ μm, $\varepsilon_r = 12.9$).

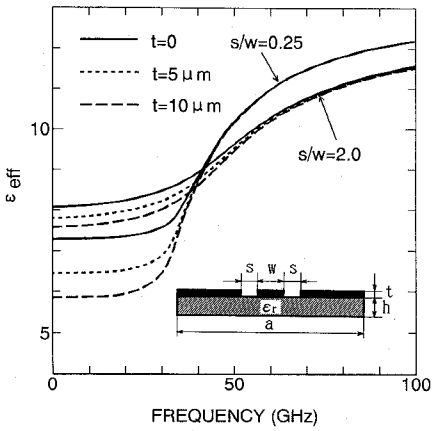

Fig. 6. Effective dielectric constants versus frequencies for a CBCPW with finite metallization thickness ($w = 72.4$ μm, $h = 0.1$ mm, $\varepsilon_r = 12.9$).

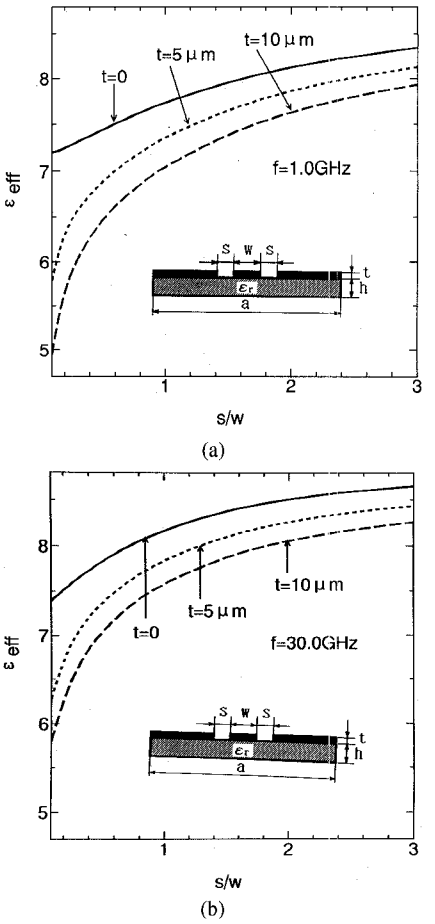

Fig. 7. Effective dielectric constants versus aperture widths for a CBCPW with finite metallization thickness ($w = 72.4$ μm, $s/w = 0.25$, $h = 0.1$ mm, $\varepsilon_r = 12.9$). (a) $f = 1$ GHz. (b) $f = 30$ GHz.

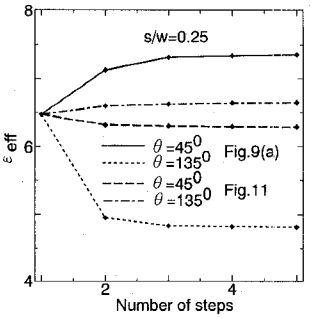

Fig. 8. Convergent diagram of the number of steps for the conductor thickness $t = 5$ μm.

where the relatively rapid increase in ε_r starts and how fast its increase speed is. A series of entire dispersion curves with different slot widths will initially be provided as follows.

Fig. 6 provides some dispersion curves for conductor-backed coplanar waveguides with strip conductor thickness $t = 0$, 5, and 10 μm for the aperture width of $s/w = 0.25$ and 2.0. Strip conductor thickness will give stronger effects on effective dielectric constants of CBCPW in the case of smaller aperture widths than large ones. At high frequencies, the effective dielectric constants with the same aperture widths are always close to the same values. The effective dielectric constants for small aperture widths are smaller than those for large aperture widths at low frequencies, but situation is reverse at high frequencies. Fig. 7 shows the effective dielectric constants versus aperture widths for strip conductor thickness $t = 0$, 5, and 10 μm at $f = 1$ GHz and 30 GHz. With the decrease of aperture widths, the effective dielectric constants for ideal zero conductor thickness will tend to a stable value. However, those for finite conductor thickness will always close to the permittivity of air region due to the concentration of electromagnetic energy into gap subregion filled with air.

For a CBCPW with the trapezoidal strip conductor cross-sections, the number of steps in a staircase approximation should be proportional to the conductor thickness for an exact modeling. For the case of relatively thin conductor thickness ($t = 5$ μm in Figs. 9–11), however, it is found from the convergent diagram as shown in Fig. 8 that a three-term staircase approximation is accurate enough to model the edge of the trapezoidal conductor.

Fig. 9 shows the dispersion curves of CBCPW with the trapezoidal strip conductor cross-sections for aperture widths $s/w = 0.25$ and 2.0. It is found that the angles of conductor edge wall affects the transmission properties in the case of $s/w = 0.25$ over the case of $s/w = 2.0$ especially at low

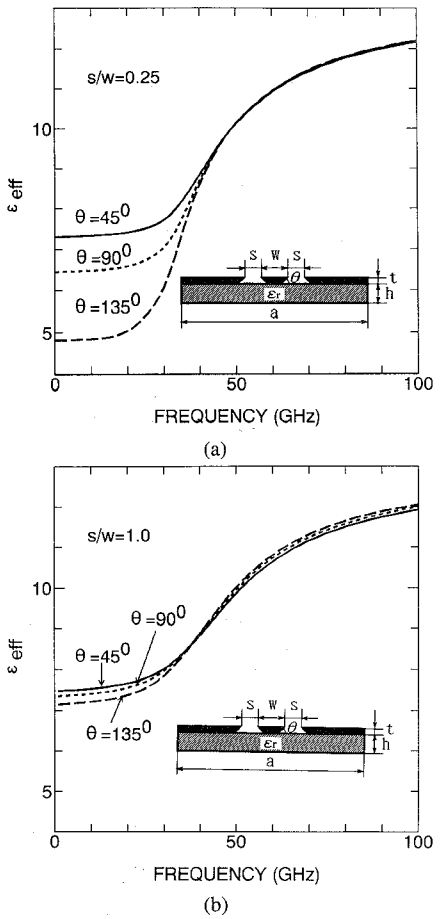

Fig. 9. Effective dielectric constants versus frequencies for a CBCPW with trapezoidal conductor cross-section ($w = 72.4$ μm, $h = 0.1$ mm, $t = 5$ μm, $\varepsilon_r = 12.9$). (a) $s/w = 0.25$. (b) $s/w = 2.0$.

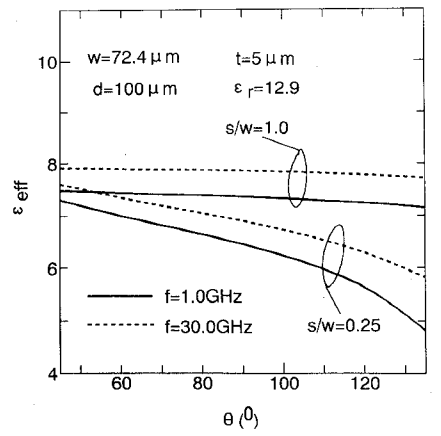

Fig. 10. Effective dielectric constants versus the angle for the structure given in Fig. 9.

frequencies. Fig. 10 provides effective dielectric constants versus angles θ with aperture widths $s/w = 0.25$ and 2.0 at $f = 1$ and 30 GHz. Figs. 9 and 10 tell us that effects of conductor edge wall angles in the small aperture widths of CBCPW must be necessarily taken into account especially at low frequencies even if conductor thickness is very small.

Fig. 11 shows dispersion curves of CBCPW with other trapezoidal strip conductor cross-sections for $s/w = 0.25$ and

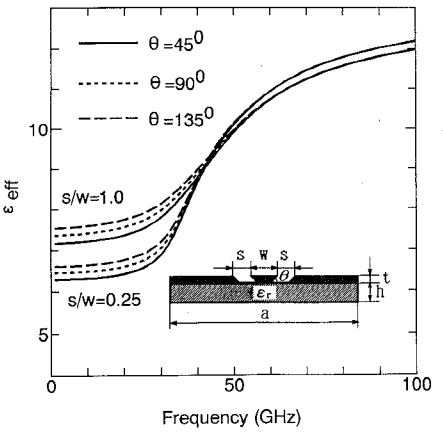

Fig. 11. Effective dielectric constants versus frequencies for a CBCPW with trapezoidal conductor cross-section ($w = \mu$ 72.4 m, $h = 0.1$ mm, $t = 5$ μm, $\varepsilon_r = 12.9$).

2.0. Aperture widths also give some effects on transmission properties but the angles of conductor edge walls produce smaller effect on transmission properties compared with the structures in Fig. 9, even in the case of small aperture widths.

Until here, dispersion characteristics of CBCPW lines with trapezoidal cross-sections have been analyzed numerically for different aperture widths. With the decrease of aperture widths, it is found that propagation constants are affected markedly by conductor edge profiles. In the case of an extremely small aperture width for CBCPW lines, a small variation of the angle of conductor strip edge walls can still bring a huge affection on propagation characteristics because of a concentration of field distributions on the aperture, which should be given a well worthwhile attention in the design of small-sized devices and components of MMIC's.

IV. Conclusion

In this paper, the boundary integral equation method was extended for the analysis of transmission properties of conductor-backed coplanar waveguides with rectangular or trapezoidal strip conductor cross-sections. Because electromagnetic fields in each subregion are expressed using an arbitrary number of Green's function series terms independently from the form of tangential fields on each aperture, this approach could shorten computation time and avoid relative convergence problems. Effects of conductor edge profile on transmission properties were discussed for different sizes of aperture width and strip conductor thickness. This Green's function method can be easily extended to study the transmission properties of planar transmission lines, such as microstrip lines and coplanar waveguides, with arbitrary conductor cross-sections and complicated multiple dielectric substrates.

Acknowledgment

The authors would like to thank Prof. K. Atsuki and Dr. N. Kishi of the University of Electro-Communications for their helpful discussions, and Mr. I. Joishi of Matsushita-Kotobuki Electronics Industries Ltd. for his support. The authors also acknowledge the reviewers for their helpful suggestions.

REFERENCES

[1] T. Itoh, "Overview of quasiplanar transmission lines," *IEEE Trans. Microwave Theory Tech.*, vol. 37, pp. 275–280, Feb. 1989.

[2] C. P. Wen, "Coplanar waveguide: A surface strip transmission line suitable for nonreciprocal gyromagnetic device applications," *IEEE Trans. Microwave Theory Tech.*, vol. MTT-17, vol. 12, pp. 1087–1090, Dec. 1969.

[3] Y. C. Shih and T. Itoh, "Analysis of conductor-backed coplanar waveguide," *Electron. Lett.*, vol. 18, no. 12, pp. 538–540, June 1982.

[4] T. Kitazawa and T. Itoh, "Asymmetrical coplanar waveguide with finite metallization thickness containing anisotropic media," in *IEEE MTT-S Int. Microwave Symp. Dig.*, 1990, pp. 673–676.

[5] J. Bornemann, "A scattering-type transverse resonance technique for the calculation of (M)MIC transmission line characteristics," *IEEE Trans. Microwave Theory Tech.*, vol. 39, pp. 2083–2088, Dec. 1991.

[6] Z. Ma, E. Yamashita, and S. Xu, "Hybrid-mode analysis of planar transmission lines with arbitrary metallization cross sections," *IEEE Trans. Microwave Theory Tech.*, vol. 41, pp. 491–497, Mar. 1993.

[7] R. Vahldieck and J. Bornemann, "A modified mode-matching technique and its application to a class of quasiplanar transmission lines," *IEEE Trans. Microwave Theory Tech.*, vol. MTT-33, pp. 916–926, Oct. 1985.

[8] R. R. Mansour and R. H. MacPhie, "A unified hybrid-mode analysis of planar transmission lines with multilayer isotropic/anisotropic substrates," *IEEE Trans. Microwave Theory Tech.*, vol. MTT-35, pp. 1382–1391, Dec. 1987.

[9] T. Kitazawa, "Analysis of shielded striplines and Finlines with finite metallization thickness containing magnetized ferrites," *IEEE Trans. Microwave Theory Tech.*, vol. 39, pp. 70–74, Jan. 1991.

[10] C. H. Chan, K. T. Ng, and A. B. Kouki, "A mixed spectral-domain approach for dispersion analysis of suspended planar transmission lines with pedestals," *IEEE Trans. Microwave Theory Tech.*, vol. 37, pp. 1716–1723, Nov. 1989.

[11] L. Zhu and E. Yamashita, "Accurate analysis of various planar transmission lines with finite metallization thickness using eigen-function weighted boundary integral equation method," *IEICE Trans. Electron.*, vol. E75-C, no. 2, pp. 259–266, Feb. 1992.

[12] ——, "Full-wave boundary integral equation method for suspended planar transmission lines with pedestals and finite metallization thickness," *IEEE Trans. Microwave Theory Tech.*, vol. 41, pp. 478–483, Mar. 1993.

[13] B. Toland and T. Itoh, "Boundary element analysis for a trapezoidal transmission line," *IEEE Microwave and Guided Wave Lett.*, vol. 1, Dec. 1991.

[14] K. A. Michalski and D. Zheng, "Rigorous analysis of open microstrip lines of arbitrary cross section in boundary and leaky regimes," *IEEE Trans. Microwave Theory Tech.*, vol. 37, pp. 2005–2010, Dec. 1989.

[15] C. J. Railton and J. P. McGeehan, "An analysis of microstrip with rectangular and trapezoidal conductor cross sections," *IEEE Trans. Microwave Theory Tech.*, vol. 38, pp. 1017–1022, Aug. 1990.

[16] C. A. Brebbia and S. Walker, *Boundary Element Techniques in Engineering*. Newnes-Butterworths, 1980.

[17] E. Yamashita and K. Atsuki, "Strip line with rectangular outer conductor and three dielectric layers," *IEEE Trans. Microwave Theory Tech.*, vol. MTT-18, pp. 238–244, May 1970.

[18] R. F. Harrington, *Time-harmonic Electromagnetic Fields*. New York: McGraw-Hill, 1961.

Lei Zhu (S'91–M'93) received the B.E. degree and the M.E. degree from the Nanjing Institute of Technology, Nanjing, China in 1985 and 1988, and the Ph.D. degree from the University of Electro-Communications, Tokyo, Japan in 1993, all in electrical engineering.

From 1986 to 1989, he was a research and teaching assistant in the Nanjing Institute of Technology, where he performed millimeter-wave components and leaky-wave antennas constructed from the groove NRD waveguide. From 1989 to 1993, he conducted studies on numerical analysis of various kinds of planar transmission lines and theoretical design of their passive components such as dividers, as a graduate student in the University of Electro-Communications. He is currently a research engineer in the Development Laboratory of Matsushita-Kotobuki Electronics Industries, Ltd., where he conducts development of various planar antennas including the phased array antenna.

Dr. Zhu received a Japanese Government (Monbusho) Graduate Fellowship during 1989 and 1993 and a First-order Achievement Award in Science and Technology from National Education Committee of China in 1993, together with four co-authors. He is also a member of the Institute of Electronics, Information and Communication Engineers of Japan.

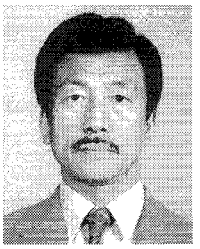

Eikichi Yamashita (M'66–SM'79–F'84) received the B.S. degree from the University of Electro-communications, Tokyo, Japan, and the M.S. and Ph.D. degrees from the University of Illinois, Urbana, all in electrical engineering, in 1956, 1963, and 1966, respectively.

From 1956 to 1964, he was a member of the research staff on millimeter-wave engineering at the Electrotechnical Laboratory, Tokyo, Japan. While on leave from 1961 to 1963 and from 1964 to 1966, he studied solid-state devices in the millimeter-wave region at the Electro-Physics Laboratory, University of Illinois. He became associate professor in 1967 and professor in 1977 in the Department of Electronic Engineering, Dean of Graduate School in 1992, the University Electro-communications, Tokyo, Japan. His research work since 1956 has been principally on applications of electro-magnetic waves such as various microstrip transmission lines, wave propagation in gaseous plasma, pyroelectric-effect detectors in the submillimeter-wave region, tunnel-diode oscillators, wide-band laser modulators, various types of optical fibers, and ultra-short electrical pulse propagation on transmission lines.

Dr. Yamashita was Chairperson of the Technical Group on Microwaves, IEICE, Japan, for the period 1985–1986 and Vice-Chairperson, Steering Committee, Electronics Group, IEICE, for the period 1989–1990. He has served as Associate Editor of the IEEE TRANSACTIONS ON MICROWAVE THEORY AND TECHNIQUES during 1980–1984. He was elected Chairperson of the IEEE Microwave Theory and Techniques Society (MTT-S) Tokyo Chapter for the period 1985–1986. He has been a member of the MTT-S ADCOM since January, 1992, and Vice-Chairperson of Chapter Operations Committee, IEEE Tokyo Section, since 1993. He served as Chairperson of International Steering Committee, 1990 Asia-Pacific Microwave Conference, held in Tokyo and sponsored by the IEICE. He edited the book, *Analysis Methods for Electromagnetic Wave Problems* (Artech House).